The Dynamic Structure Factor of LiC_6 and KC_8: Inelastic Synchrotron X-Ray Scattering Results*

A. Berthold, K.-J. Gabriel, and W. Schülke

Institute of Physics, University of Dortmund, Fed. Rep. of Germany

Z. Naturforsch. **48a**, 283–288 (1993); received December 30, 1991

The dynamic structure factor $S(\boldsymbol{q}, \omega)$ of electrons in lithium-intercalated graphite (LiC_6) and potassium-intercalated graphite (KC_8) for momentum transfer $\boldsymbol{q} \parallel c$-axis has been measured by inelastic synchrotron X-ray scattering. The dielectric function $\varepsilon(\boldsymbol{q}, \omega)$ was deduced from the data and compared with $\varepsilon(\boldsymbol{q}, \omega)$ of pristine graphite.

The main feature in the different $\mathrm{Im}[\varepsilon(\boldsymbol{q}, \omega)]$-spectra, a more or less intense peak around 14 eV, can be assigned to maxima of the symmetry-projected joint density of occupied and unoccupied electron states near the Fermi level. Knowing the position of the occupied bands by photoemission experiments, predictions about the unoccupied π and interlayer states can be made.

In the case of LiC_6, a shift and broadening of the first $\mathrm{Im}[\varepsilon(\boldsymbol{q}, \omega)]$-peak was found, which can be explained by a decrease of the energy of the interlayer-band because of the strong hybridization of this graphite-derived band with the Li metal 2s-band.

In the case of KC_8, a weakening of the first peak of $\mathrm{Im}[\varepsilon(\boldsymbol{q}, \omega)]$ was observed, which we attribute both to a decreasing overlap of the occupied π-derived state with the empty interlayer state and to a change of symmetry of the occupied σ-derived states as well as of the empty π-derived states.

Key words: Inelastic X-ray scattering; Dynamic structure factor; Graphite; Graphite intercalation compounds; Interlayer state.

1. Introduction

The graphite intercalation compounds (GICs) have been the object of great controversial discussions in recent years.

The so-called interlayer state, first predicted by Posternak et al. [1], exhibits high electron density between the graphite layers and forms a band with strong k_z-dispersion close to the Fermi energy.

The existence of this state in pure graphite, not correlated to the presence of alkali atoms, required a new interpretation of the origin of a band, present close to E_F in alkali-metal GICs, which was attributed to alkali *s*-electrons. This band has to be understood now as a hybrid of alkali s-electrons and the graphite interlayer state [2].

Regarding LiC_6, it is commonly accepted that this interlayer state is located completely above the Fermi level, but the exact energetic position of this band is just a point of theoretical [3, 4] and experimental [5–7] investigations.

On the other hand, concerning KC_8, it is an unanswered question which amount of charge of the additional valence electron is transferred from potassium to previously empty carbon π-states upon intercalation and whether a potassium 4s-like three-dimensional Fermi surface in the centre of the Brillouin zone exists. For a detailed list of experimental and theoretical studies see [8].

Inelastic X-ray scattering spectroscopy (IXSS) can help to answer some of the open questions because of the band-structure information this method is providing.

The remainder of our paper is organized as follows. In the next two sections we give a short survey about the fundamentals and the experimental setup of IXSS. After some information about graphite and its intercalation compounds we discuss the experimental results of our measurements for graphite, LiC_6 and KC_8. A short conclusion is given at the end.

2. IXSS – Inelastic X-Ray Scattering Spectroscopy

The basic idea of IXSS [9] is to measure the double-differential cross-section (DDCS) $\frac{\mathrm{d}^2\sigma}{\mathrm{d}\omega\,\mathrm{d}\Omega}$ in order to get information about the dynamic structure factor

* Presented at the Sagamore X Conference on Charge, Spin, and Momentum Densities, Konstanz, Fed. Rep. of Germany, September 1–7, 1991.

Reprint requests to Prof. Dr. W. Schülke, Institute of Physics, University of Dortmund, P.O.B. 50 05 00, D-W-4600 Dortmund 50, Fed. Rep. of Germany.

0932-0784 / 93 / 0100-0283 $ 01.30/0. – Please order a reprint rather than making your own copy.

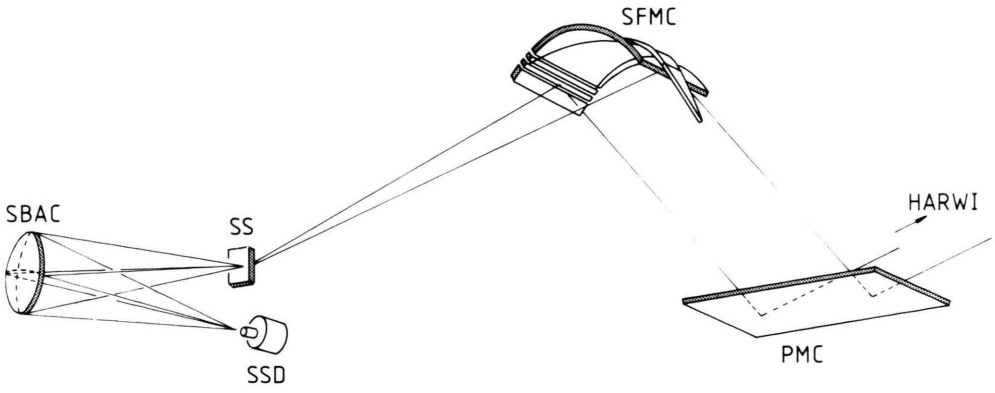

Fig. 1. Experimental setup for IXSS at the wiggler-beamline of HASYLAB at DESY, Hamburg.
PMC Plane Monochromator Crystal, SBAC Spherically Bent Analysing Crystal,
SFMC Sagitally Focussing Monochromator Crystal, SSD Solid-State Detector.
SS Scattering Sample,

$S(\boldsymbol{q}, \omega)$ of the scattering electron system,

$$\frac{\mathrm{d}^2\sigma}{\mathrm{d}\omega\,\mathrm{d}\Omega} = (\boldsymbol{e}_1 \cdot \boldsymbol{e}_2)^2\, r_0^2\, \frac{\omega_2}{\omega_1}\, S(\boldsymbol{q}, \omega)\,, \tag{1}$$

where $\hbar\omega = \hbar(\omega_1 - \omega_2)$ is the energy and $\hbar\boldsymbol{q} = \hbar(\boldsymbol{q}_1 - \boldsymbol{q}_2)$ is the momentum transferred to the scattering system, if the incoming photon with energy $\hbar\omega_1$, momentum $\hbar\boldsymbol{q}_1$ and polarization $\boldsymbol{e}_1$ is scattered into a photon with energy $\hbar\omega_2$, momentum $\hbar\boldsymbol{q}_2$ and polarization $\boldsymbol{e}_2$, respectively. r_0 is the classical electron radius.

The dynamic structure factor $S(\boldsymbol{q}, \omega)$ is the Fourier transform in time of the ground-state expectation value of the correlation between scattering phases of electrons at different times,

$$S(\boldsymbol{q}, \omega) = \frac{1}{2\pi} \int \mathrm{d}t\, e^{i\omega t} \langle I | \sum_{jj'} e^{-i\boldsymbol{q}\cdot\boldsymbol{r}_j(t)}\, e^{i\boldsymbol{q}\cdot\boldsymbol{r}_{j'}(0)} | I \rangle\,. \tag{2}$$

$S(\boldsymbol{q}, \omega)$ is connected with the dielectric-response function $\varepsilon^{-1}(\boldsymbol{q}, \omega)$ by means of the fluctuation-dissipation theorem,

$$S(\boldsymbol{q}, \omega) = -\frac{\hbar^2 q^2}{4\pi^2 e^2 n}\, \mathrm{Im}\,[\varepsilon^{-1}(\boldsymbol{q}, \omega)]\,, \tag{3}$$

where n is the electron density.

If we represent the electron states of the scattering system by one-electron Bloch states with wave vector $\boldsymbol{k}$, band index ν, energy $E(\boldsymbol{k}, \nu)$ and Fermi function $f_0(\boldsymbol{k}, \nu)$, the imaginary part of the dielectric function $\mathrm{Im}\,[\varepsilon(\boldsymbol{q}, \omega)]$, which is accessible from the IXSS-data by Kramers–Kronig transformation, provides band-structure information in a rather direct way:

$$\mathrm{Im}\,[\varepsilon(\boldsymbol{q}, \omega)] = -\left(\frac{4\pi e^2}{q^2}\right) \sum_{\boldsymbol{k}, \nu, \boldsymbol{k}', \nu'} |\langle \boldsymbol{k}', \nu' | e^{i\boldsymbol{q}\cdot\boldsymbol{r}} | \boldsymbol{k}, \nu \rangle|^2$$
$$\times \{f_0(\boldsymbol{k}', \nu') - f_0(\boldsymbol{k}, \nu)\}\, \delta(\hbar\omega + E(\boldsymbol{k}, \nu) - E(\boldsymbol{k}', \nu'))\,. \tag{4}$$

According to (4), $\mathrm{Im}\,[\varepsilon(\boldsymbol{q}, \omega)]$ reflects, via the sum over δ-functions, the joint density of states (JDOS), which connects occupied with unoccupied one-electron states. The squared transition-matrix element $\langle \boldsymbol{k}', \nu' | e^{i\boldsymbol{q}\cdot\boldsymbol{r}} | \boldsymbol{k}, \nu \rangle$ produces symmetry projections off the JDOS.

3. IXSS – Experimental Setup

The experimental setup is shown schematically in Figure 1. We use synchrotron X-radiation from the HARWI wiggler-beamline, monochromatized to a primary energy of about 14 keV by use of a Si-[5,1,1] fixed-exit double-crystal monochromator with sagittally focussing second crystal. The analyser consists of a spherically bent Si-[12,0,0] crystal, reflecting the scattered radiation under a Bragg-angle of 86°, which leads to a fixed analysed energy of 13.7 keV. The spectral analysis was done by varying the primary energy.

4. Scattering Samples

Graphite consists of hexagonal layers with a nearest-neighbour distance of 1.42 Å; the separation between

adjacent carbon layers is 3.35 Å. There are two inequivalent types of carbon atoms per unit cell [10]. The graphite sample we used was a highly oriented pyrolytic-graphite disc of 2 mm thickness.

Graphite intercalation compounds (GIC) [11] are formed by insertion of atomic or molecular layers between the layers of a graphite host material. The GICs are classified by a stage index n denoting the number of graphite layers between adjacent intercalate layers.

Stage-1 lithium-intercalated graphite (LiC_6) has been prepared by a liquid-phase reaction under Ar atmosphere. The lithium atoms are arranged midway between two carbon layers such that one-third of the C hexagons have Li atoms directly above and below. The carbon layers are stacked in registry (A–A stacking), in contrast to graphite, which has an A–B-type stacking. The distance between carbon layers is increased in LiC_6 to 3.706 Å [3]. The sample thickness was 2 mm.

Stage-1 potassium-intercalated graphite KC_8 has been prepared by the two-zone vapour transport method. One potassium atom lies above the centre of each fourth carbon hexagon. Adjacent carbon layers are in registry again, separated by 5.35 Å; there exist two inequivalent carbon sites with respect to their potassium neighbourhood [12]. The thickness of the sample we used was ca. 0.5 mm.

5. Experimental Results

The sample mounting allows momentum transfer $\boldsymbol{q} \parallel c$-axis and $\boldsymbol{q} \perp c$-axis, where the crystalline c-axis is perpendicular to the carbon layer. In this experiment only momentum transfers $\boldsymbol{q} \parallel c$-axis were realized with different values of q between 0.59 a.u. and 1.67 a.u.

Considering the symmetry projections owing to the transition matrix element, the number of possible transitions is restricted. Within the limits of the dipole approximation, where the scattering operator $e^{i\boldsymbol{q}\cdot\boldsymbol{r}}$ is replaced by $i\boldsymbol{q}\cdot\boldsymbol{r}$, the dipole-allowed transitions with momentum transfer $\boldsymbol{q} \parallel c$-axis are from occupied π-bands to unoccupied σ-bands and vice versa. These transitions correspond to nearly-parallel-band situations in band structure plots of the $k_{x,y}$-dispersion.

5.1. Graphite

In Fig. 2 and Fig. 3 the $S(\boldsymbol{q}, \omega)$-spectra of pristine graphite together with calculated $\mathrm{Re}[\varepsilon(\boldsymbol{q}, \omega)]$- and $\mathrm{Im}[\varepsilon(\boldsymbol{q}, \omega)]$-spectra are shown in the upper part of each picture.

The first peak in $\mathrm{Im}[\varepsilon(\boldsymbol{q}, \omega)]$ has been attributed to two kinds of transitions [13], namely transitions between the occupied σ-band and the nearly parallel unoccupied π-band with energy losses around 16 eV and between the occupied π-band and the unoccupied σ-type interlayer-band with energy losses around 14 eV. The latter becomes possible because of the considerable extension of the π-states into the interlayer region.

Both of these contributions to the first peak are only slightly separated in energy so that they could not be resolved experimentally. A double-peak structure of this type was also predicted by Chen and Rabii [14].

5.2. LiC_6

$S(\boldsymbol{q}, \omega)$-spectra of LiC_6, together with the deduced $\mathrm{Re}[\varepsilon(\boldsymbol{q}, \omega)]$- and $\mathrm{Im}[\varepsilon(\boldsymbol{q}, \omega)]$-spectra, are presented in Fig. 2 (lower part of each picture).

The first peak in the $\mathrm{Im}[\varepsilon(\boldsymbol{q}, \omega)]$-spectra is shifted by 2–3 eV to lower energies upon intercalation with Li; the FWHM increases.

In order to explain this behaviour we consider again the two kinds of transitions:

Because of the nearly rigid-band behaviour both of the occupied σ-band [15] and of the unoccupied π-band (see our core excitation spectroscopy results [16]) we conclude that the energy of the $\sigma \rightarrow \pi$-transition remains roughly the same.

In contrast to that, the energy of the $\pi \rightarrow \sigma$-type interlayer state transition is shifted down to lower values. Whereas the occupied π-band shows rigid-band behaviour [15], the interlayer band of LiC_6 will be 2 eV lower in energy than the graphite interlayer state, possibly because of strong hybridization with the Li metal 2s-band [2].

This non-rigid band shift of the interlayer state with respect to all other bands is in very good agreement both with experimental results by Fauster et al. [5] (ARIPE: energy shift of 1.4 eV) and with band structure calculations by Holzwarth et al. [4], who predict an energy shift of 1.6 eV.

5.3. KC_8

The $S(\boldsymbol{q}, \omega)$-data of potassium-intercalated graphite are shown in Figure 3.

In contrast to our LiC_6-results, the first peak in the $\mathrm{Im}[\varepsilon(\boldsymbol{q}, \omega)]$-spectra is very strongly reduced upon in-

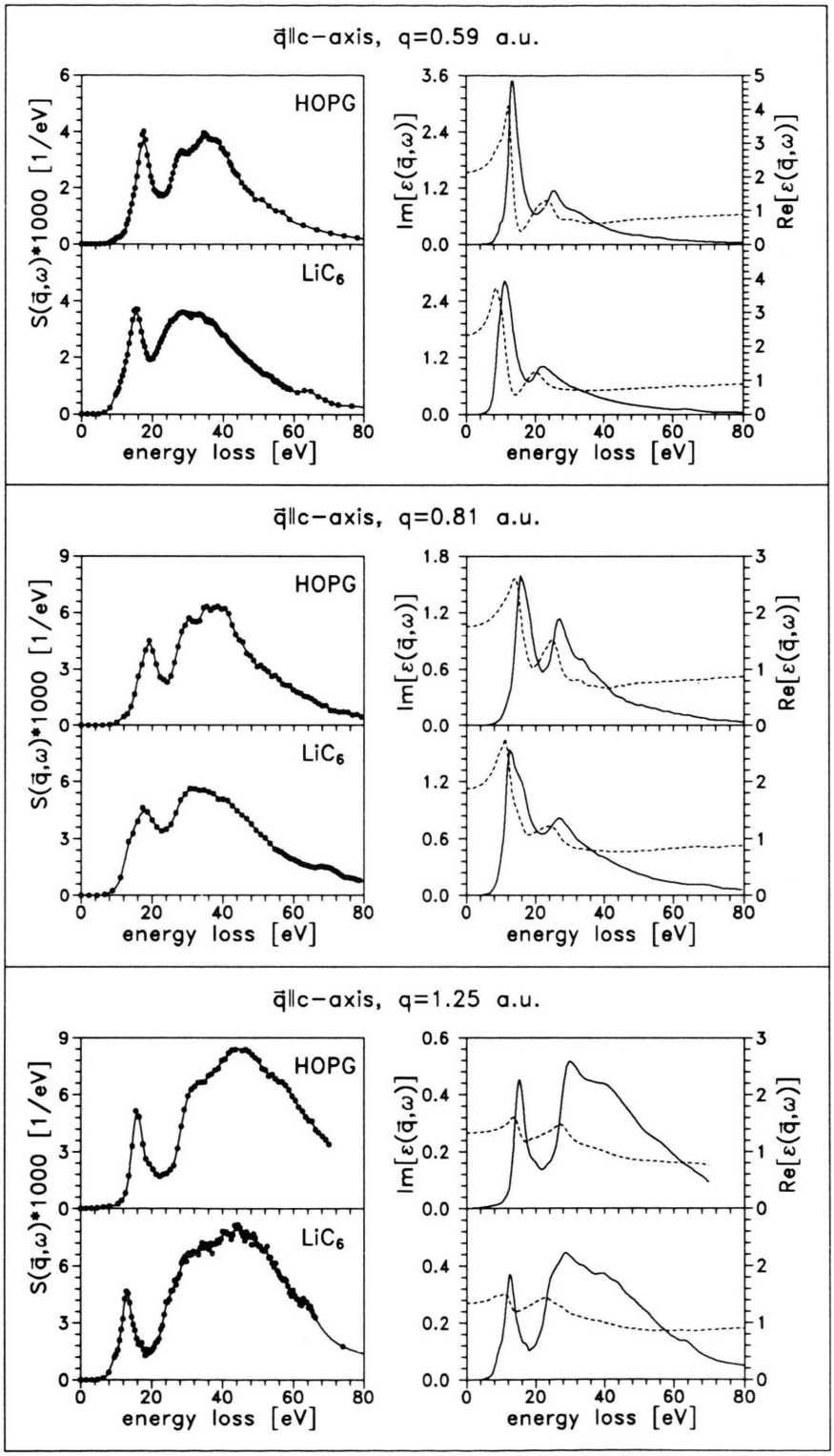

Fig. 2. *Left-hand side:* $S(\boldsymbol{q}, \omega)$ of highly oriented pyrolytic graphite (upper part of each picture) and LiC_6 (lower part of each picture). *Right-hand side:* Calculated $\mathrm{Re}[\varepsilon(\boldsymbol{q}, \omega)]$ (dashed curve, right-hand scale) and $\mathrm{Im}[\varepsilon(\boldsymbol{q}, \omega)]$ (solid line, left-hand scale) of HOPG and LiC_6 by means of Kramers–Kronig transformation.

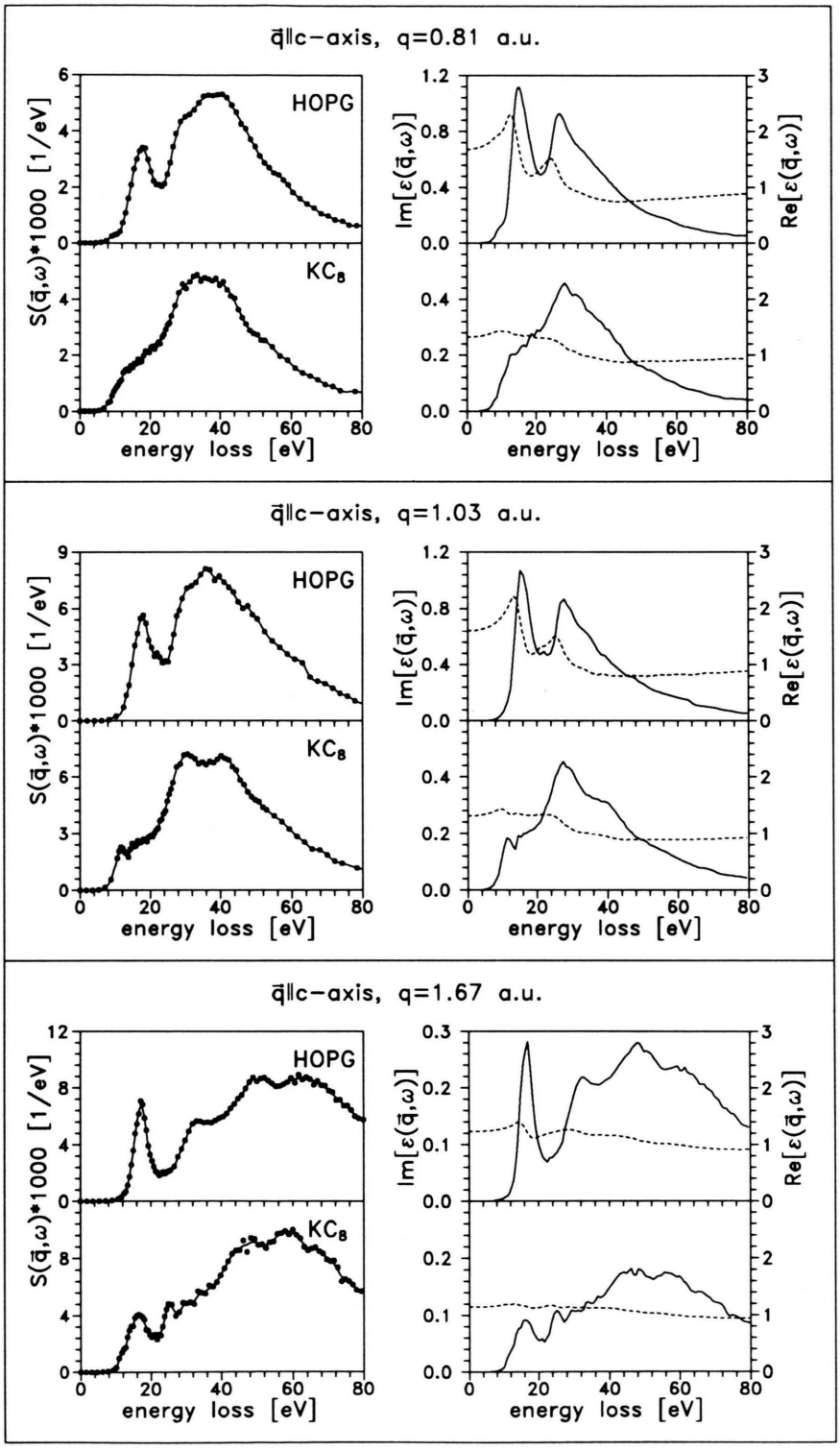

Fig. 3. *Left-hand side:* $S(\boldsymbol{q}, \omega)$ of highly oriented pyrolytic graphite (upper part of each picture) and KC_8 (lower part of each picture). *Right-hand side:* Calculated $\mathrm{Re}[\varepsilon(\boldsymbol{q}, \omega)]$ (dashed curve, right-hand scale) and $\mathrm{Im}[\varepsilon(\boldsymbol{q}, \omega)]$ (solid line, left-hand scale) of HOPG and KC_8 by means of Kramers–Kronig transformation.

tercalation. This peak becomes a weak shoulder for smaller q-values, starting at somewhat lower energies, and diminishes to a small bump left at the same position as in pristine graphite for larger qs.

Again the behaviour of the two contributions to this peak has to be analysed [17]:

Owing to the increasing carbon-layer distance, the overlap between the π-orbitals of carbon and the centre of the interlayer state, which is located midway between the layers, is highly diminished. So we conclude a nearly complete disappearance of the $\pi \rightarrow$ interlayer-state transition. The remaining transition seems to have its onset at ≈ 10.5 eV. Knowing from ARUPS [18] that the position of the non-backfolded occupied π-band is 9.5 eV below E_F at the Γ-point, this onset would mean a lower limit of 1 eV above E_F for the Γ-point of the interlayer state.

Calculated results for the interlayer-state position at the Γ-point are 2.5 eV (Mizuno et al. [19]) and 1.5 eV above E_F (Di Vincenzo and Rabii [12]); photoyield experiments [20] find 2.6 eV, and EELS [21] gives 2.2 eV above E_F.

Concerning the $\sigma \rightarrow \pi$-transition, a weakening of this contribution to the first peak of $\mathrm{Im}[\varepsilon(\boldsymbol{q}, \omega)]$ without appreciable energy shift could be observed. Analysing band structure calculations, a change of symmetry of the carbon-derived states upon intercalation can be seen [12], whereas the relative energy separation of the bands remains more or less untouched. Reasons for these variations are changes of the crystal structure (from D_{6h}^6 in graphite to D_{2h}^{24} in KC_8) and of the local environment of the carbon atom (two inequivalent carbon sites with respect to their potassium neighbourhood in KC_8). A group-theoretical analysis yields a reduction of the number of dipole-allowed $\sigma \rightarrow \pi$-transitions for $\boldsymbol{q} \parallel c$-axis by 50% for transitions at the M-point and by nearly 90% for transitions at the Γ-point.

If the π-derived $\Gamma_{1,2}^-$ states of KC_8 were pushed below E_F, as predicted by the band-structure calculation of Mizuno et al. [22], the allowed transitions would be further reduced.

The energy position of the residual peak at 15 eV is in reasonable agreement with calculations [12], where 16 eV for the $\Gamma_1^+ \rightarrow \Gamma_2^-$-transition was found.

6. Conclusions

In conclusion, we have presented $\varepsilon(\boldsymbol{q}, \omega)$-data calculated from our IXSS-measurements and explained the origin and nature of the first peak in the $\mathrm{Im}[\varepsilon(\boldsymbol{q}, \omega)]$-spectra both for graphite and the two kinds of GICs, using dipole selection rules. We could show that the interlayer-state, which is originally graphite-like, lowers in energy upon intercalation, but does not intersect the Fermi level. In KC_8, a strong reduction of the transition probability owing to structural changes could be observed.

Acknowledgements

We thank H.-J. Güntherodt and V. Thommen-Geiser from the University of Basel, Switzerland, for valuable help with the sample preparation. This work has been funded by the German Federal Ministry of Research and Technology (BMFT) under Contract No. 05 434AXB.

[1] M. Posternak, A. Baldereschi, A. J. Freeman, E. Wimmer, and M. Weinert, Phys. Rev. Lett. **50,** 761 (1983).
[2] N. A. W. Holzwarth, S. G. Louie, and S. Rabii, Phys. Rev. B **30,** 2219 (1984).
[3] N. A. W. Holzwarth, S. Rabii, and L. A. Girifalco, Phys. Rev. B **18,** 5190 (1978).
[4] N. A. W. Holzwarth, S. G. Louie, and S. Rabii, Phys. Rev. B **28,** 1013 (1983).
[5] Th. Fauster, F. J. Himpsel, J. E. Fischer, and E. W. Plummer, Phys. Rev. Lett. **51,** 430 (1983).
[6] I. Schäfer, M. Schlüter, and M. Skibowski, Phys. Rev. B **35,** 7663 (1987).
[7] F. Maeda, T. Takahashi, H. Ohsawa, S. Suzuki, and H. Suematsu, Phys. Rev. B **37,** 4482 (1988).
[8] W. Schülke, K.-J. Gabriel, A. Berthold, and H. Schulte-Schrepping, Sol. State Comm. **79,** 657 (1991).
[9] W. Schülke, Nucl. Instr. Meth. A **280,** 338 (1989).
[10] R. C. Tatar and S. Rabii, Phys. Rev. B **25,** 4126 (1982).
[11] M. S. Dresselhaus and G. Dresselhaus, Adv. Phys. **30,** 139 (1981).
[12] D. P. Di Vincenzo and S. Rabii, Phys. Rev. B **25,** 4110 (1982).
[13] W. Schülke, U. Bonse, H. Nagasawa, A. Kaprolat, and A. Berthold, Phys. Rev. B **38,** 2112 (1988).
[14] N.-X. Chen and S. Rabii, Phys. Rev. B **31,** 4784 (1985).
[15] W. Eberhardt, I. T. McGovern, E. W. Plummer, and J. E. Fischer, Phys. Rev. Lett. **44,** 200 (1980).
[16] W. Schülke, A. Berthold, A. Kaprolat, and H.-J. Güntherodt, Phys. Rev. Lett. **60,** 2217 (1988).
[17] W. Schülke, A. Berthold, H. Schulte-Schrepping, K.-J. Gabriel, V. Thommen-Geiser, and H.-J. Güntherodt, Sol. State Comm. **79,** 661 (1991).
[18] T. Takahashi, N. Gunasekara, T. Sagawa, and H. Suematsu, J. Phys. Soc. Japan **55,** 3498 (1986).
[19] S. Mizuno, H. Hiramoto, and K. Nakao, Sol. State Comm. **63,** 705 (1987).
[20] C. F. Hague, G. Indlekofer, U. M. Gubler, P. Oelhafen, H.-J. Güntherodt, and J. Schmidt-May, Sol. State Comm. **48,** 1 (1983).
[21] J. J. Ritsko and C. F. Brucker, Sol. State Comm. **44,** 889 (1982).
[22] S. Mizuno, H. Hiramoto, and K. Nakao, J. Phys. Soc. Japan **56,** 4466 (1987).